N

LBL-9874

CONF-790917--19

Lawrence Berkeley Laboratory
UNIVERSITY OF CALIFORNIA

Materials & Molecular Research Division

MASTER

Presented at the American Chemical Society Conference,
Washington, D. C., September 9-14, 1979

SYNTHESIS AND CHARACTERIZATION OF Pa(IV), Np(IV), AND Pu(IV) BOROHYDRIDES

Rodney H. Banks and Norman M. Edelstein

December 1979

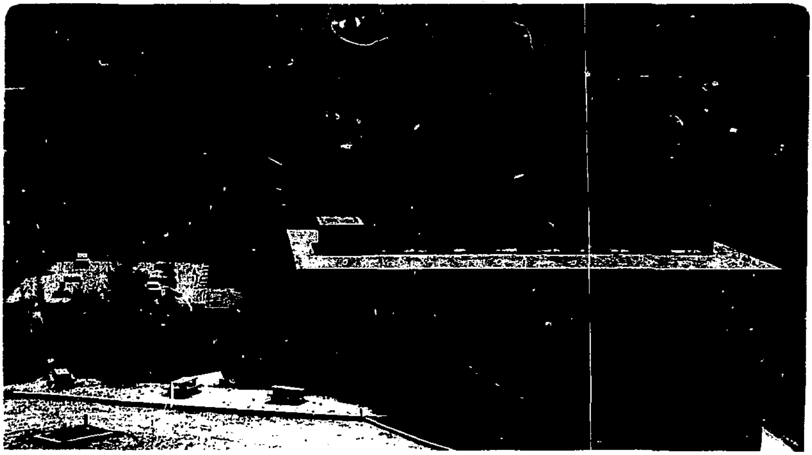

Prepared for the U.S. Department of Energy under Contract W-7405-ENG-48

LBL-9874

SYNTHESIS AND CHARACTERIZATION OF Pa(IV), Np(IV), AND Pu(IV) BOROHYDRIDES

Rodney H. Banks and Norman M. Edelstein

Materials and Molecular Research Division, Lawrence
Berkeley Laboratory, Berkeley, California 94720
and
Department of Chemistry, University of California,
Berkeley, California 94720

Abstract

The actinide borohydrides of Pa, Np, and Pu have been prepared and some of their physical and optical properties measured. X-ray powder diffraction photographs of $Pa(BH_4)_4$ have shown that it is isostructural to $Th(BH_4)_4$ and $U(BH_4)_4$. $Np(BH_4)_4$ and $Pu(BH_4)_4$ are much more volatile than the borohydrides of Th, Pa, and U and are liquids at room temperature. Results from low-temperature single-crystal x-ray diffraction investigation of $Np(BH_4)_4$ show that its structure is very similar to $Zr(BH_4)_4$. With the data from low-temperature infrared and Raman spectra, a normal coordinate analysis on $Np(BH_4)_4$ and $Np(BD_4)_4$ has been completed. EPR experiments on $Np(BH_4)_4/Zr(BH_4)_4$ and $Np(BD_4)_4/Zr(BD_4)_4$ have characterized the ground electronic state.

Introduction

Four of the seven known metal tetrakis-borohydrides--Zr, Hf, Th, and U borohydrides (1,2)--were first synthesized about 30 years ago during the Manhattan project. They were found to be very volatile and reactive compounds. In recent years, much structural, spectroscopic, and chemical studies were done on these molecules. New tetrakis-borohydrides of the actinides Pa, Np, and Pu have recently been prepared by analogous reactions used in the syntheses of U and Th borohydrides (3). The Pa compound, $Pa(BH_4)_4$, is isomorphous to and behaves like $U(BH_4)_4$ and $Th(BH_4)_4$ while x-ray studies on $Np(BH_4)_4$ and the isostructural $Pu(BH_4)_4$ have shown that they resemble the highly volatile Zr and Hf compounds both in structure and properties. All seven compounds contain triple hydrogen bridge bonds connecting the boron atom to the metal. The 14 coordinate Th, Pa, and U borohydrides (4), in addition, have double-bridged borohydride groups that are involved in linking metal atoms together in a low symmetry, polymeric structure. The structures of the other four borohydride molecules are monomeric and much more symmetrical; the 12 coordinate metal is surrounded by a tetrahedral array of BH_4^- groups (5,6,7).

In an effort to understand the energy level structures of actinide 4+ ions in borohydride environments, optical and magnetic measurements have been initiated. Spectra of pure $Np(BH_4)_4$ and $Np(BD_4)_4$, and these compounds diluted in single-crystal host matrices of $Zr(BH_4)_4$ and $Zr(BD_4)_4$, respectively, have been obtained in the region 2500-300 nm at 2K. The covalent actinide borohydrides display rich vibronic spectra (8) and assignment of the observed bands depends on a knowledge of the vibrational energy levels of $M(BH_4)_4$ molecules. A normal coordinate analysis derived from low-temperature infrared and Raman spectra of $Np(BH_4)_4$ and $Np(BD_4)_4$ was undertaken to elucidate the nature of their fundamental vibrations and overtones. Electron paramagnetic resonance (epr) spectra of $Np(BH_4)_4$ and $Np(BD_4)_4$ that characterize the ground electronic state have been obtained in a number of host materials. Optical spectra of $Pa(BH_4)_4$ and $Pa(BD_4)_4$ isolated in an organic glass were obtained in the near infrared and visible regions at 2K. This paper will summarize our progress to date on these studies.

Experimental

Preparation of Borohydrides. Metal borohydrides are very chemically reactive and most of them are pyrophoric in air. The syntheses of the compounds and all manipulations with Al, Zr, Hf, Np, and Pu borohydrides must therefore be performed in a grease-free high-vacuum line. Work involving the less volatile Th, Pa, and U borohydrides can also be done in argon-filled dryboxes.

All actinide borohydrides are made by reacting the anhydrous actinide tetrafluoride with liquid $Al(BH_4)_3$ in the absence of a solvent in a sealed glass reaction tube. The basic reaction equation is:

$$AnF_4 + 2Al(BH_4)_3 \rightarrow An(BH_4)_4 + 2AlF_2BH_4.$$

Purification of the desired product is accomplished by sublimation where only the unreacted $Al(BH_4)_3$ and $An(BH_4)_4$ are volatile. The large difference in volatilities of these compounds permit easy separation. $Th(BH_4)_4$ and $Pa(BH_4)_4$ are obtained on a 0° cold finger by heating the solid reaction mixture to 120° and 55°, respectively. Uranium, neptunium, and plutonium borohydrides sublime at room temperature and are collected in a dry ice trap through which the $Al(BH_4)_3$ passes into a liquid nitrogen trap. The stabilities of the actinide borohydrides dictate the type of reaction conditions needed for successful preparation. The polymeric compounds are stable at room temperature and their syntheses are carried out at 25° for about five days. $Np(BH_4)_4$ and $Pu(BH_4)_4$ are unstable at room temperature and require that the tetrafluorides react at 0° for only a few hours. These two borohydrides must be stored at dry-ice or liquid-nitrogen temperature in a greaseless storage tube. $Zr(BH_4)_4$ used in experiments described here was prepared similarly to $U(BH_4)_4$ by reacting Na_2ZrF_6 with $Al(BH_4)_3$.

Preparation of Borodeuterides. All glassware which contacts the borodeuterides had been previously passivated with B_2D_6 or treated with D_2O and then baked out thoroughly under vacuum. The borodeuterides of Th, Pa, and U are prepared as described above using $Al(BD_4)_3$ as the source of BD_4^-. The high volatilities of the covalent borohydrides allow their deuterated analogs to be prepared by a more satisfactory method that utilizes the $H \leftrightarrow D$ exchange property of these molecules with deuterium (9). If the D_2 gas is maintained in large excess, the extent of equilibrium will give the fully deuterated product in high yield. In a passivated glass bulb, a mixture of the borohydride vapor and 1 atm of D_2 gas was allowed to stand for a few days at room temperature. After freezing out the products at -78° and evacuating, another volume of D_2 was added and the exchange reaction continued. Three cycles were sufficient to give the metal borodeuteride having an isotopic purity as high as that of the deuterium used (99.7%).

An attempt to prepare $Np(BT_4)_4$ using the above method resulted in the decomposition of the borohydride due to the extremely high radiation field of the T_2 gas (66 Ci) and no volatile Np compound was recovered.

The vapor pressure of $Np(BH_4)_4$ was determined as a function of temperature using a Bourdon gauge (5). The data for the liquid and solid shown in Figure 1 were used in calculating thermodynamic quantities of the actinide borohydrides given in Table 1. A single crystal x-ray study (5) was carried out for $Np(BH_4)_4$ at 130K. Its structure is shown in Figure 2.

Gas-phase infrared and low-temperature solid-state infrared and Raman spectra were obtained for $Np(BH_4)_4$ and $Np(BD_4)_4$ from 2.5 to 50μ. Assignments were made of the observed bands and the fundamental frequencies were fitted to calculated values in a normal coordinate analysis (10).

Electron paramagnetic resonance spectra were taken of $Np(BH_4)_4/Zr(BH_4)_4$ and $Np(BD_4)_4/Zr(BD_4)_4$ mixed crystals at X, K, and Q bands. Spin Hamiltonian parameters were found by a least-squares fit of the data.

Electronic spectra of $Pa(BH_4)_4$ and $Pa(BD_4)_4$ in an organic glass were obtained at 2K from 2200 nm - 300 nm.

Results and Discussion

The crystal structure of $U(BH_4)_4$ has been examined by single crystal x-ray (4b) and neutron diffraction techniques (4a). Much like the bonding in the well-known boron hydrides (11), this metal borohydride exhibits hydrogen bridge bonds that join the boron atom to the metal. In $U(BH_4)_4$, there are two tridentate and four bidentate BH_4^- groups. The tridentate bridge bond links the metal atom to the boron atom through a triple-hydrogen-bridge bond while the fourth hydrogen atom forms a terminal bond with the boron atom. The bidentate bridge bond links one boron atom to two metal atoms through two double-hydrogen-bridge bonds, resulting in a helical polymeric structure.

Low-temperature x-ray powder diffraction photographs(3) of $Np(BH_4)_4$ and $Pu(BH_4)_4$ revealed that they are isostructural and of a unique structure type. The structure of $Np(BH_4)_4$ was determined by a low-temperature, single-crystal x-ray study at 130K (5). The borohydride molecules are monomeric and crystallize into the tetragonal space group, $P4_2/nmc$, where a = 8.559(9) Å, c = 6.017(9) Å, and Z = 2. The four terminal, triply-bridged borohydride groups are bound to the Np atom with Np–B distances of 2.46(3) Å. Although the hydrogen atoms were observed in the Fourier maps and refined, values of the $Np{\cdot}H_b$ bond lengths, 2.2(5) Å, had large standard deviations. No evidence was found for symmetry lower than T_d for $Np(BH_4)_4$.

The molecular structure of $Np(BH_4)_4$ is illustrated in the ORTEP diagram shown in Figure 2.

Structural studies on $Zr(BH_4)_4$ (6) and $Hf(BH_4)_4$ (7) have shown that these molecules are monomeric and crystallize into a cubic lattice with molecular structures very similar to those of Np and Pu borohydrides.

Some of the physical properties of metal tetrakis-borohydrides, which are primarily determined by their solid-state structure, are listed in Table 1. The polymeric Th, Pa, and U borohydrides are of much lower volatility than the monomeric Zr, Hf, Np, and Pu compounds. The intermolecular bonds connecting molecules together decrease their volatility substantially since these bonds break when the solid vaporizes (12). A plot of log p(mmHg) vs 1/T yields the equation log p(mmHg) = –A/T + B, where T is in K. Values of A and B allow the calculation of the heats (ΔH) and entropies (ΔS) for phase-change processes as shown in Table 1. The actinide ions in the polymeric compounds are 14 coordinate; however, in the gaseous state they are 12 coordinate (12).

The free energy for the structure transformation at 290K described by the equation

$U(BH_4)_4$ (solid, 14 coordinate, 4 double hydrogen bridge bonds, 2 triple-hydrogen-bridge bonds)

$\rightarrow U(BH)_4)_4$ (solid, 12 coordinate, 4 triple hydrogen bridge bonds)

can be estimated. ΔH and ΔS values for a 12 coordinate $U(BH_4)_4$ structure were obtained by an extrapolation of the measured quantities for $Hf(BH_4)_4$ and $Np(BH_4)_4$ vs metal ionic radius. Subtracting these derived $U(BH_4)_4$ values from the corresponding measured ones gives the heat of transformation (4.5 Kcal/mol) and entropy of the transformation (6.5 cal/mol degree) of the 14 coordinate to the 12 coordinate structure for $U(BH_4)_4$. Using the equation $\Delta G = \Delta H - T\Delta S$, ΔG is found to be +2.6 Kcal/mol. This value can be compared to the free energy of an exchange process involving the bridge and terminal hydrogen atoms in solution for $(C_5H_5)_3UBH_4$ where $\Delta G^* \approx 5$ Kcal/mol at the coalescence temperature of $-140 \pm 20^\circ$C (13). The calculated value for the spontaneous transformation of the 14 coordinate structure to the 12 coordinate structure is ∿700K.

In addition to low vapor pressure, high melting points and low solubility in noncoordinating organic solvents are characteristic of the polymeric borohydrides. In contrast, Zr, Hf, and Np borohydrides melt around room temperature and are highly soluble in pentane.

Vibrational Spectroscopy. In spite of their complex molecular frameworks, the monomeric borohydrides display surprisingly simple vibrational spectra due to their high symmetry (T_d), which requires that many fundamental vibrations be degenerate. Normal coordinate analyses have been carried out for $Zr(BH_4)_4$ (14) and $Hf(BH_4)_4$ (15) and a similar study was completed for $Np(BH_4)_4$ in order to compare vibrational energy level structures and elucidate the nature of the fundamental vibrations of $Np(BH_4)_4$ (10). Table 2 lists the measured frequencies. The appendix compares our notation to that of earlier work (7b,15). Unless otherwise specified, the ^{11}B isotope is implied.

A tetrahedral $M(BH_4)_4$ molecule has 57 normal modes of vibration which are divided into five symmetry types, $4A_1 + A_2 + 5E + 5T_1 + 9T_2$. The nine T_2 modes are infrared active and the $4A_1$ (polarized), 5E, and $9T_2$ modes are Raman active. Those vibrations of T_1 and A_2 symmetry are both infrared and Raman inactive.

νBH_t stretching motions transform as $A_1 + T_2$ and these are seen in the highest frequency regions 2600-2500 cm^{-1} (1950-1900 cm^{-1}) for the borohydride (borodeuteride). The 12 BH_b bonds (stretches) transform as $A_1 + E + T_1 + 2T_2$ and modes involving these coordinates occur at 2200-1900 cm^{-1} (1600-1500 cm^{-1}). The next region of fundamental activity, 1300-1100 cm^{-1} (1000-800 cm^{-1}), consists of normal modes composed of νMH_b stretches and δHBH bends, with each symmetry equivalent set classified as $A_1 + E + T_1 + 2T_2$. Modes consisting mainly of νMB stretches occur at lower energies, 600-450 cm^{-1} (500-400 cm^{-1}). The lowest frequency vibrations are observed below 200 cm^{-1} and involve δHMH and δBMB bends. In addition to the fundamental vibrations, overtones and combination bands are also seen. Peaks due to ^{10}B and ^1H (in the deuteride spectra) are resolved in the solid-state, low-temperature spectra.

The gas-phase infrared spectra for $Np(BH_4)_4$ and $Np(BD_4)_4$ are shown in Figure 3. The frequencies and assignments for the bands are given in Table 2. The solid-state spectra show many more bands and it is from these that a normal coordinate analysis was carried out.

A modified valence force field using the force constants and internal coordinates listed in Table 3 gave the calculated frequencies shown with the corresponding observed ones in Table 4. The force constants are very similar to those used in $Zr(BH_4)_4$ and $Hf(BH_4)_4$ even though the force fields are slightly different. The significant VMB force constant implies that there may be some direct metal-boron bonding in these borohydrides. The force field obtained for $Np(BH_4)_4$ is consistent for a molecule intermediate in covalency between that in diborane (16) and the alkali borohydrides (17).

Electron Paramagnetic Resonance. EPR spectroscopy involves transitions within the magnetic sublevels of the ground electronic state of a metal ion in the GHz energy region. The $^4I_{9/2}$ ground state of the Np^{4+} ion in a T_d crystal field of the form

$$V = B_4[C_0^{(4)} + (5/14)^{1/2}(C_4^{(4)} + C_{-4}^{(4)})] + B_6[C_0^{(6)} - (7/2)^{1/2}(C_4^{(6)} + C_{-4}^{(6)})]$$

splits into an isotropic Γ_6 doublet and two anisotropic Γ_8 quartets. Isotropic spectra for $Np(BH_4)_4$ and $Np(BD_4)_4$ establish the Γ_6 level as the ground state. The spin Hamiltonian describing the system is

$$\mathcal{H} = AI\cdot S' + g\beta H\cdot S' - g_I\beta H\cdot I ,$$

where A is the hyperfine coupling constant, I = 5/2 for ^{237}Np, and S' = 1/2. The calculations were carried out using $|F, m_F\rangle$ basis sets where F = I + S'. In zero magnetic field there are two states, F = 2 and F = 3, that are separated by 3A. When the magnetic field is turned on, each of these two states splits into $(2F + 1)|m_F\rangle$ levels as shown in Figure 4 where A is assumed positive. The arrows in Figure 4 represent observed allowed transitions.

Results of least-squares calculations of the data to the spin-Hamiltonian above are shown in Table 5. The $Np(BH_4)_4/Zr(BH_4)_4$ spectra gave relatively broad resonances compared to the deuteride and a reliable g_I value could not be found. Inclusion of a nonzero g_I value in the calculations of the deuteride data improved the fit even though it was calculated to be very small. However, the significance of this improved fit must be tested further. Similar trials on the hydride data gave poorer fits.

The experimental g value is lower than calculated from LLW wavefunctions (17) (∿2.7), which may indicate that covalency (19) or Jahn-Teller (20) effects may be important.

Electronic Spectra of $Pa(BH_4)_4$. Cary 17 spectra of $Pa(BH_4)_4$ and $Pa(BD_4)_4$ in an organic glass at 2K are shown in Figure 5.

In liquid solution at 25° C, the dissolved $Pa(BH_4)_4$ is monomeric and of T_d symmetry. Under these conditions there are five crystal field levels: Γ_7, Γ_8, and Γ_6, Γ_7', Γ_8' of the $^2F_{5/2}$ (ground) and $^2F_{7/2}$ levels. Point charge calculations (20) give the $\Gamma_8(^2F_{5/2})$ level as the ground state.

Keiderling (7b) has observed that when $U(BH_4)_4$ dissolved in an organic solvent is cooled to 2K, the monomeric T_d structure transforms back into the polymeric structure. Although it is tempting to assign the observed bands based upon the tetrahedral structure, definite conclusions must await comparison with pure $Pa(BH_4)_4$ spectra.

Near infrared and optical spectra have been obtained for $Np(BH_4)_4$ and $Np(BD_4)_4$ diluted in $Zr(BH_4)_4$, $Zr(BD_4)_4$ and methylcyclohexane at 2K. The spectra are dominated by vibronic transitions and the analysis of the data is now underway.

Summary

The actinide borohydrides $Pa(BH_4)_4$, $Np(BH_4)_4$, and $Pu(BH_4)_4$ have been synthesized. The structure of $Np(BH_4)_4$ has been studied by single-crystal x-ray diffraction and found to be similar in structure to $Hf(BH_4)_4$. A normal coordinate analysis on $Np(BH_4)_4$ was completed using IR and Raman spectra. The electronic ground state of $Np(BH_4)_4$ has been characterized by EPR spectroscopy. The electronic spectra of $Np(BH_4)_4$ and $Pa(BH_4)_4$ are under investigation.

Acknowledgment

This work was done with support from the Division of Nuclear Sciences, Office of Basic Energy Sciences, U.S. Department of Energy, under Contract No. W-7405-Eng-48.

Literature Cited

1. Hoekstra, H.R.; Katz, J.J. J. Am. Chem. Soc., 1949, 71, 2488.

2a. Schlesinger, H.I.,: Brown, H.C. J. Am. Chem. Soc., 1953, 75, 219.

2b. Katz, J.J.; Rabinowitch, E. "Chemistry of Uranium"; McGraw-Hill: New York NY, 1951.

3. Banks, R.H.; Edelstein, N.M.; Rietz, R.R.; Templeton, D.H.; Zalkin, A. J. Am. Chem. Soc., 1978, 100, 1975.

4a. Bernstein, E.R.; Hamilton, W.C.; Keiderling, T.A.; LaPlaca, S.J.; Lippard, S.J.; Mayerle, J.J. Inorg. Chem., 1972, 11, 3009.

4b. Bernstein, E.R.; Keiderling, T.A.; Lippard, S.J.; Mayerle, J.J. J. Am. Chem. Soc., 1972, 94, 2552.

5. Banks, R.H.; Edelstein, N.M.; Spencer, B.; Templeton, D.H.; Zalkin, A. J. Am. Chem. Soc., 1980, 102, 0000.

6. Bird, P.H.; Churchill, M.R. Chem. Comm., 1967, 403.

7a. Broach, R.S.;Chuang, I.S.; Williams, J.M.; Marks, T.J. Private communication, 1979.

7b. Keiderling, T.A. PhD thesis, Princeton University, 1974.

8. Bernstein, E.R.; Keiderling, T.A. J. Chem. Phys., 1973, 59, 2105.

9. Maybury, P.C.; Larrabee, J.C. Abstract of papers, 135th Meeting of the American Chemical Society, 1959. P-28M.

10. Banks, R.H.; Edelstein, N.M., to be published.

11. Muetterties, E.L. "Boron Hydride Chemistry"; Academic Press: New York NY, 1975.

12. James, B.D.; Smith, B.E.; Wallbridge, M.G.H. J. Mol. Struct. 1972, 14, 327.

13. Marks, T.J.; Kolb, J.R. J. Am. Chem. Soc., 1975, 97, 27.

14. Smith, B.E.; Shurvell, H.F.; James, B.D. JCS Dalton, 1978, 710.

15. Keiderling, T.A.; Wozniak, W.T.; Gay, R.S.; Jurkowitz, D.; Bernstein, E.R.; Lippard, S.J.; Spiro, T.G. Inorg. Chem., 1975, 14, 576.

16. Price, W.C. J. Chem. Phys., 1948, 16, 894.

17. Emery, A.R.; Taylor, R.C. J. Chem. Phys., 1958, 28, 1029.

18. Bleany, B. Proc. Roy. Soc. Lond., 1964, A277, 289.

19. Judd, B.R. 2nd Inter. Conf. on Electronic Structure of An, Warsaw, Poland, 1976.

20. Lea, K.R.; Leask, M.J.M.; Wolf, W.P. J. Phys. Chem. Solids, 1962, 23, 1381.

Table 1
Physical Properties of Metal Tetrakis-Borohydrides

Property	$Th(BH_4)_4$[a]	$U(BH_4)_4$[b]	$Hf(BH_4)_4$[a]	$Zr(BH_4)_4$[a]	$Np(BH_4)_4$[c]
Crystallographic space group	$P4_32_12$ (tetragonal)	$P4_32_12$[d] (tetragonal)	$P\overline{4}3m$[e] (cubic)	$P\overline{4}3m$[f] (cubic)	$P4_2/nmc$ (tetragonal)
Solid-state structure	polymeric	polymeric	monomeric	monomeric	monomeric
Density in the solid state(gm/cc)	2.53	2.69	1.85	1.13	2.23
Melting point (°C)	203[g]	126[g]	29.0	28.7	14.2
Boiling point (°C) extrap.	-	-	118	123	153
Vapor pressure (mmHg/°C)	0.05/130	0.19/30	14.9/25	15.0/25	10.0/25
Liquid[h] A	-	-	2097	2039	1858
Liquid B	-	-	8.247	8.032	7.24
Solid[h] A	-	4264.6	2844	2983	3168
Solid B	-	13.354	10.719	10.919	11.80
Heat of sublimation (Kcal/mol)	21	19.5	13.0	13.5	14.5
Heat of vaporization (Kcal/mol)	-	-	9.6	9.3	8.5
Heat of fusion (Kcal/mol)	-	-	3.4	4.3	6.0
Entropy of sublimation (cal/mol°)	-	61.1	49.0	50.0	54.0
Entropy of vaporization (cal/mol°)	-	-	37.7	36.8	33.1
Entropy of fusion (cal/mol°)	-	-	11.3	13.2	20.9
Solubility in pentane	insol	slight	high	high	high

[a] Ref. 1

[b] Ref. 2

[c] Ref. 5

[d] Ref. 4

[e] Ref. 7

[f] Ref. 6

[g] With decomposition

[h] $\log p(mmHg) = -A/T + B$

Table 2

Observed Bands in Gas-Phase IR Spectra of $Np(BH_4)_4$ and $Np(BD_4)_4$

Energy (cm^{-1})	Assignment	Internal coordinates	Comments
$Np(BH_4)_4$			
2568	$\nu_1^{T_2}$	νBH_t	strong
2480	$2\nu_4^{T_2}, 2\nu_5^{T_2}$		weak, v.br.
2350	$\nu_{4,5}^{T_2} + \nu_6^{T_2}$		weak, br.
2155	$\nu_2^{T_2}$	νBH_b	strong
2130	$2\nu_3^{T_1}$		sh on $\nu_5^{T_2}$
2084	$\nu_3^{T_2}$	νBH_b	strong, sharp
1280			sh on $\nu_4^{T_2}, \nu_5^{T_2}$
1240	$\nu_4^{T_2}$, $\nu_5^{T_2}$	$\delta HBH, \nu MH_b$	strong, broad
1205			sh on $\nu_4^{T_2}, \nu_5^{T_2}$
1122	$\nu_6^{T_2}$	$\delta HBH, \nu MH_b$	medium, sl.br.
1080	$\nu_4^{T_2} - \nu_5^{E}$		sh on $\nu_6^{T_2}$
478	$\nu_8^{T_2}$	νMB, νMH_b	strong
$Np(BD_4)_4$			
1930		$\nu ^{10}BD_t$	sh on $\nu_1^{T_2}$
1922	$\nu_1^{T_2}$	νBD_t	strong
1605	$2\nu_3^{T_1}$ *		medium
1562		$\nu ^{10}BD_b$	sh on $\nu_2^{T_2}$
1558	$\nu_2^{T_2}$ *	νBD_b	strong
1526	$\nu_3^{T_2}$	νBD_b	strong,sharp
1190		δHBD	v.weak, br.
928	$\nu_4^{T_2}, \nu_5^{T_2}$	$\delta DBD, \nu MD_b$	strong, sl.br
845	$\nu_6^{T_2}$	$\delta DBD, \nu MD_b$	weak, br.
437	$\nu_7^{T_2}$	νMB, νMD_b	strong

In the table: br = broad, sh = shoulder, sl = slightly, v = very, H_b = bridging hydrogen, H_t = terminal hydrogen. (See Appendix for description of notation)

*These two bands are apparently in Fermi resonance.

Table 3

Best Fit Force Constants for Solid Neptunium Borohydride at 77K

Primary Force Constants		Interaction Force Constants	
Internal coordinate	Value	Internal coordinates	Value
νBH_t	3.51 md/Å	$\nu BH_b:\nu BH_b$ (intra)	.04 md/Å
νBH_b	2.36	$\nu MH_b:\nu MH_b$	.02
νMH_b	.37	$\nu MB:\delta H_bMH_b$	-.09 md/rad
νMB	1.28	$\nu BH_b:\delta H_bBH_b$ (intra)	.04
δH_tBH_b	.28 mdÅ/rad^2	$\nu MH_b:\delta H_bMH_b$	.04
$\delta H_b..L_b(C_3)$	.26		
δH_bBH_b	.36		
ϵH_bBMB	.18*		

* This force constant was arbitrarily set at .18 since this depends almost solely on the A_2 torsion mode, which is not observed.

Table 4

Fundamental Vibrations (cm^{-1}) of $Np(BH_4)_4$ and $Np(BD_4)_4$

Mode	$Np(BH_4)_4$		$Np(BD_4)_4$	
	Observed	Calculated	Observed	Calculated
$\nu_1^{T_2}$	2551	2557	1912	1911
$\nu_2^{T_2}$	2143	2144	1548	1603
$\nu_3^{T_2}$	2069	2078	1516	1485
$\nu_4^{T_2}$	1247	1266	926	897
$\nu_5^{T_2}$	1225	1223	917	895
$\nu_6^{T_2}$	1138	1104	860	824
$\nu_7^{T_2}$	—	575	437	447
$\nu_8^{T_2}$	475	488	—	415
$\nu_9^{T_2}$	130	156	112	139
$\nu_1^{A_1}$	2557	2554	1913	1905
$\nu_2^{A_1}$	2149	2147	1517	1523
$\nu_3^{A_1}$	1283	1284	955	953
$\nu_4^{A_1}$	517	517	475	466
ν_1^{E}	2123	2117	1619	1589
ν_2^{E}	1260	1270	905	899
ν_3^{E}	1053	1089	795	807
ν_4^{E}	—	571	—	413
ν_5^{E}	168	142	154	125
$\nu_1^{T_1}$	—	2116	—	1587
$\nu_2^{T_1}$	—	1256	—	889
$\nu_3^{T_1}$	—	1084	—	810
$\nu_4^{T_1}$	—	565	—	405
$\nu_5^{T_1}$	—	405	—	288
ν^{A_2}	—	268	—	204

Table 5

Electron Paramagnetic Resonance of $^{237}Np(BH_4)_4$ and $^{237}Np(BD_4)_4$

$$\mathcal{H} = A\mathbf{I}\cdot\mathbf{S}' + g\beta\mathbf{H}\cdot\mathbf{S}' - g_I\beta\mathbf{H}\cdot\mathbf{I} \quad \begin{matrix} I=5/2 \\ S'=1/2 \end{matrix}$$

Spin Hamiltonian Parameters

	$\lvert A\rvert$ (cm^{-1})	g	g_I
$Np(BH_4)_4$	.1140 ± .001	1.894 ± .002	∼0
$Np(BD_4)_4$	.1140 ± .001	1.892 ± .002	.0062 ± .002

Observed and Calculated Field Values (gauss) at K Band

$Np(BH_4)_4$ ν = 25.986GHz		$Np(BD_4)_4$ ν = 24.238GHz	
Observed	Calculated	Observed	Calculated
6355.6	6355.8	5683.1	5683.1
7295.0	7294.3	6596.0	6595.8
8406.0	8405.7	7695.0	7694.3
9700.0	9700.2	8991.0	8991.4
11177.0	11178.1	10487.6	10487.1
12829.6	12828.7	12167.9	12167.6

Figure Captions

Figure 1. Vapor pressure vs 1/T for $Np(BH_4)_4$. The open circles represent data of the liquid and the solid circles are those for the solid.

Figure 2. ORTEP diagram of $Np(BH_4)_4$.

Figure 3. Gas phase infrared spectra of $Np(BH_4)_4$ and $Np(BD_4)_4$.

Figure 4. Observed allowed epr transitions for $Np(BH_4)_4$/$Zr(BH_4)_4$. X band —·—· K band —— Q band ----

Figure 5. Optical spectra of $Pa(BH_4)_4$ and $Pa(BD_4)_4$ in methylcyclohexane. S above a peak represents a solvent band.

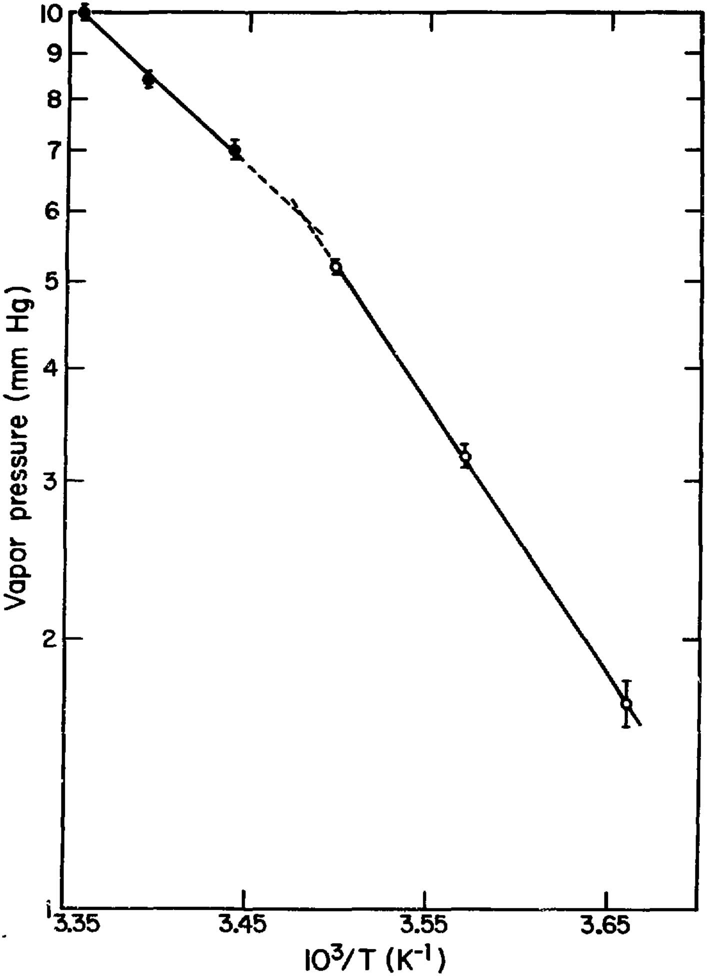

XBL 796-1725

Figure 1

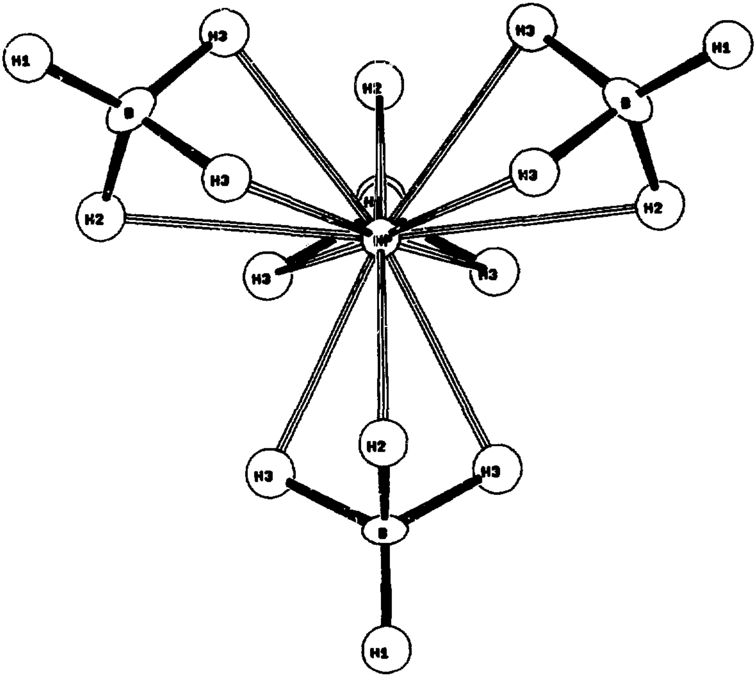

XBL 795-9592

Figure 2

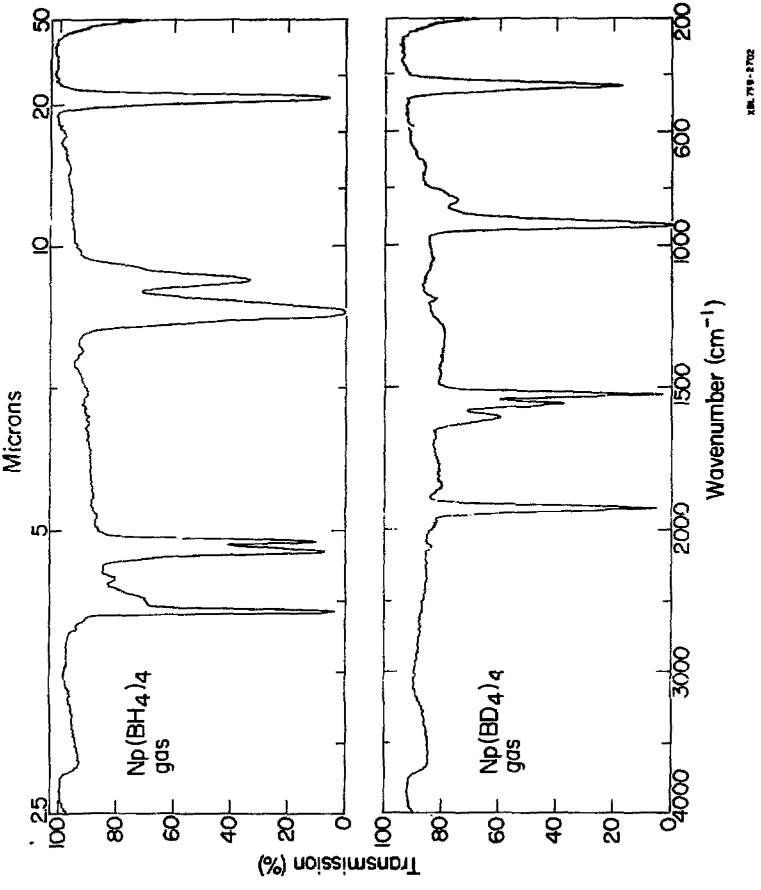
Microns
2.5
5
10
20
50
Np(BH$_4$)$_4$
gas
Np(BD$_4$)$_4$
gas
Transmission (%)
100
80
60
40
20
0
4000
3000
2000
1500
1000
600
200
Wavenumber (cm^{-1})
XBL 759-2702

Figure 3

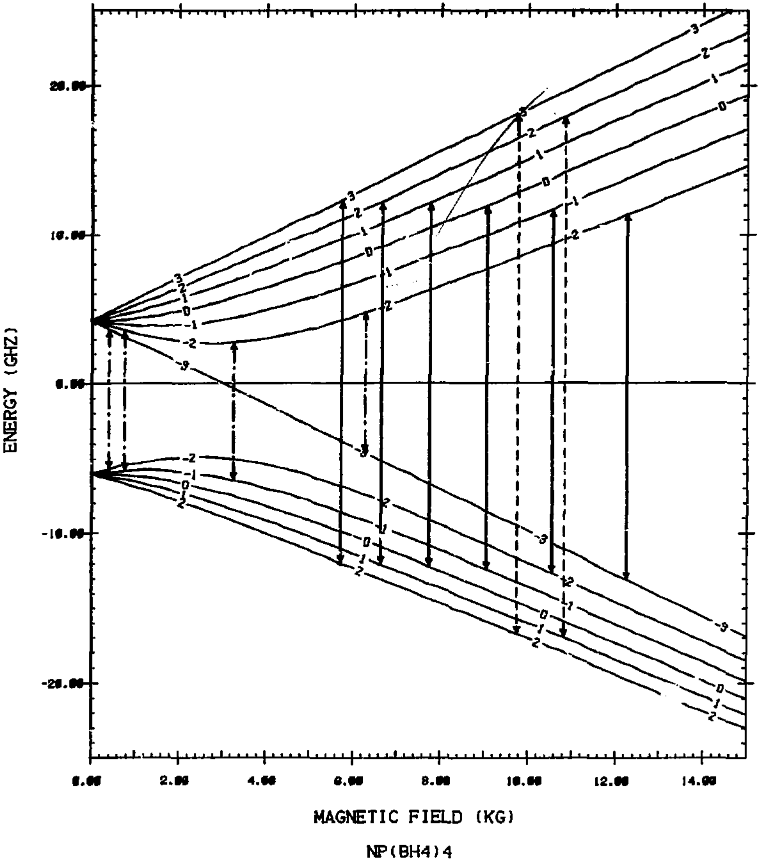

XBL 798-11097

Figure 4

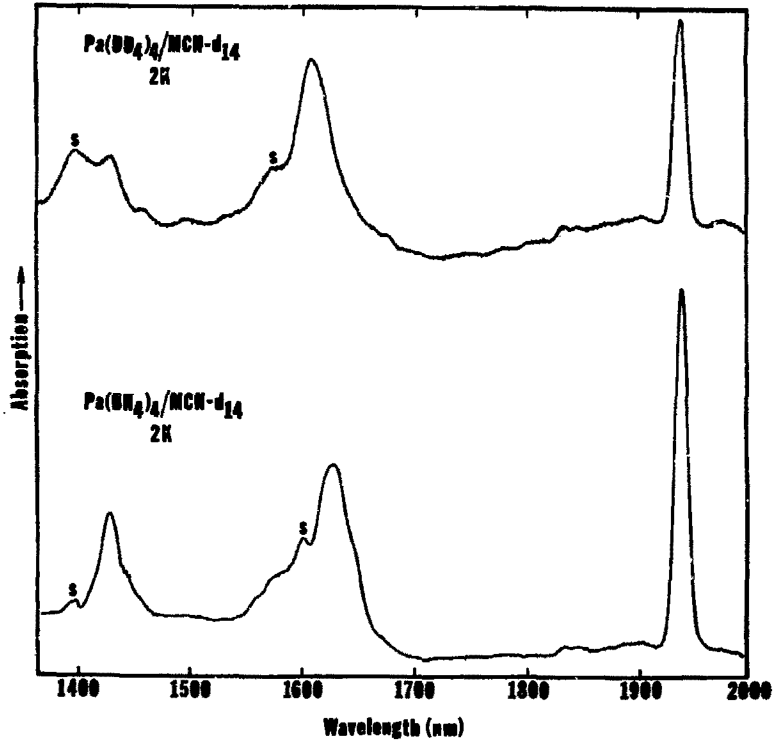

XBL 798-11146

Figure 5